

Hepcat Report: Year 1

Zoë Smith

April 2024

1 Introduction

Exploration into dark matter searches necessitating meV-scale resolution involves the study of phonon-mediated interactions. SuperCDMS has demonstrated the feasibility of Phonon-Mediated Transition Edge Sensor (TES) based detectors achieving eV-scale energy resolution, as evidenced by their work (see, for example, [6]). Despite the longstanding success of TES-based detectors, challenges in fabrication and scalability, particularly concerning the production of over 10,000 detectors, have spurred investigations into alternative technologies to achieve meV-scale sensitivity.

The DMQIS group at SLAC that I am a member of is exploring a range of new technologies that could achieve sensitivity to the meV-scale regime, including RF-multiplexed sensors. I lead our work on superconducting Microwave Kinetic Inductance Detectors (MKIDs). MKID devices, whose operation was first demonstrated by Day, have found increasing utility across various sensing applications over the past two decades ([1, 9]). These offer a promising solution, being relatively straightforward to fabricate and enabling simpler scalability for achieving meV-scale sensing thresholds. They are also a simple system for probing film quality as our group explores lower T_c films than Al for a range of sensing applications.

Kinetic Inductance Phonon-Mediated (KIPM) detectors are calorimetric devices using an MKID to readout phonon energy deposited in to the crystal. Recent advancements have reached resolution levels of O(100 eV), rivaling TES-based phonon sensors [5, 8, 2, 7]. These detectors typically comprise a superconducting coplanar waveguide (CPW) and a thin-film lumped-element resonator on a crystalline substrate.

Operationally, these detectors require cooling well below the transition temperature of the resonator film. Phonons propagating through the crystal are absorbed in the film and break cooper pairs. The sensitivity of the detector is impacted by the gap of the thin film used to pattern the resonator. This increases quasi-particle density, changing the complex surface impedance of the superconducting film. This change in surface impedance shifts the resonant frequency downward, which can be tracked via transmission measurements through the CPW. The additional metallization needed for reading out the sensitive detector volume, including the CPW and capacitor, presents a challenge in terms of signal loss. Efforts are underway to mitigate these impacts, with recent low-threshold devices achieving only 0.85% energy efficiency, compared to 10% for higher-coverage designs ([5, 7], and 30% in TES-based designs ([6]).

In the first year of my HEPCAT fellowship, I have focused on building fabrication and readout infrastructure for KIPM based detectors to be studied at SLAC, that will also be used for the SQUAT ([3]) sensors our group is developing. This report will encompass discussions on the fabrication considerations and progress for KIPM detectors and phonon sensitive TES detectors, along with considerations in KIPM detector design, RF-HV housing design, and preliminary testing of KIPMs at SLAC.

2 Fabrication and Process Testing

I have developed fabrication processes at SLAC/Stanford for KIPM detectors using a variety of deposition tools and etch techniques. Images of the devices at various points in the fabrication process are shown in figure 2. Typical fabrication processes first patterns thin film aluminum to create the resonator, and then patterns the wiring using niobium. The process development for MKIDS has covered 3 rounds of fabrication, with a 4th round ongoing. A summary of the 4 fabrication runs is included in table 1.

Fab Run	Device Format	Films Used	Results
1	Slim and Square Chips	Al/Nb	No Al resonator yield, but Niobium resonators with $Q_r = 40,000$
2	Square Chips (1cm)	Al/Nb	No yield of resonators. Aluminum film destroyed during Niobium processing, which was over-etched.
3	Square Chips (1cm)	Al (30nm and 45nm)	Very low-Q aluminum resonators ($Q_r = 1700$). Tc of 1.4 K.
4	Square Chips and DC Test Features	Al & AlMn	TBD

Table 1: Fabrication runs thus far. See text and table for more details.

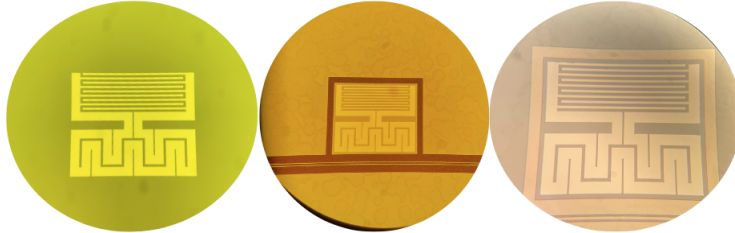


Figure 1: Images of Al resonators throughout the fabrication of the KIPM detectors. Left: Post Al etch, Center: Post Nb etch, Right: Post photoresist plasma clean.

Aluminum films are deposited using either sputtering systems or e-beam evaporators. Niobium films are deposited in an e-beam evaporator. Patterning uses a Heidelberg MLA-150 direct write tool to enable rapid changes in mask designs. To etch, I have used both wet and dry etches. Dry etches have the benefit of being more reproducible between users, are an easier entry point for beginners in fabrication, and do avoid direct access with dangerous chemicals. Dry etch recipes can also be tuned to create straight side wall, maintaining the desired area contact of your device and the substrate. In addition to developing a dry etch recipe for KIPM detectors at SLAC/Stanford, I developed a dry etch recipe for HVeV detectors. I have found some downsides for dry etching, however. To start, the dependency on heavily used equipment results in frequent tool failure and contamination. Dry etchants also attack the silicon substrate, and it is unclear the effects this will have on phonon collection efficiency. Additionally, dry etching heats photoresist making it difficult to remove. This often requires an Oxygen plasma clean to remove the photoresist.

Finally, wet etching thin aluminum films can be combined with the development of the photoresist, since TMAH-based developers is an aluminum etchant. This simplifies fabrication of aluminum devices drastically.

3 Film Characterization

In order to better diagnose the loss of Aluminum resonators in the first and second rounds of fabrication, I took a closer look at the effects of the fabrication process on the film quality.

3.1 Tc Testing

To better understand the effects of the fabrication process on our aluminum film quality, I investigated the transition temperature and residual resistance ratio (RRR) at various points in the fabrication process using both sputtered and evaporated aluminum films. Tc measurements were done using 4-wire measurements in a dilution refrigerator. The measured values are shown in Tab. 2. In both the sputtered and evaporated films, subsequent processing increased the transition temperatures and lowered the RRR, with the greatest drop in tested RRR coming after the O_2 plasma etch to remove photoresist. While decreasing RRR is an indicator of increased impurities, the sputtered aluminum film transitioned after the O_2 plasma clean. This indicates

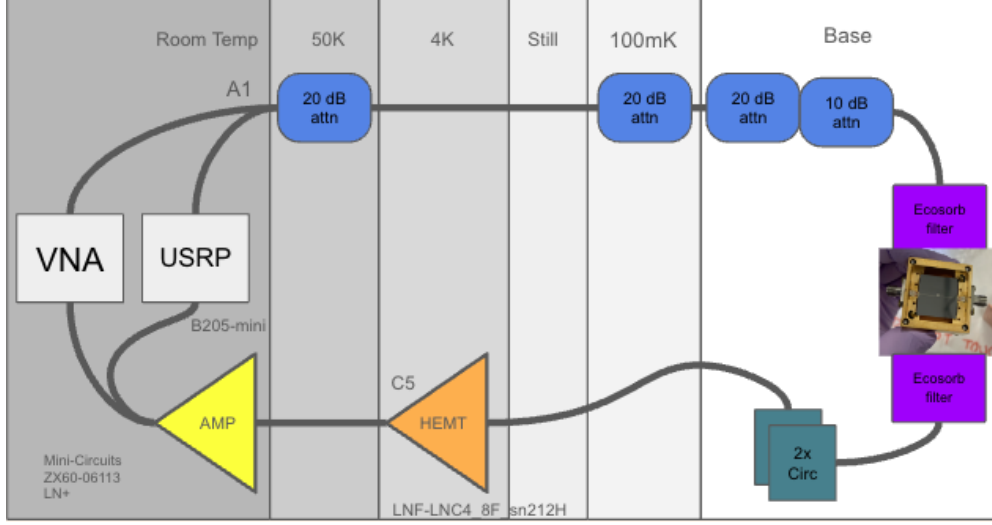


Figure 2: A typical cryostat setup for a KIPM detector. Readout is preformed using a vector network analyzer (VNA) or software defined radio.

that the loss of aluminum conductivity in the second round of fabrication occurred during the second round of photo lithography.

	30 nm Sputtered Al		30 nm Evaporated Al	
Last completed step in fabrication process	T _c (K)	RRR	T _c (K)	RRR
Deposit 30 nm Al	—	—	1.346 ± 0.005	3.31 ± 0.02
Develop PR in MF26A	1.36 ± 0.01	6.74 ± 0.02	1.37 ± 0.03	2.49 ± 0.04
Dry etch Al & wet removal of PR	1.36 ± 0.01	5.08 ± 0.02	—	—
Dry etch Al, wet removal of PR & O ₂ plasma ash of PR	1.405 ± 0.006	2.56 ± ±0.02	—	—

Table 2: Transition temperatures and RRR of aluminum samples after various steps in the process. “—” indicates no samples were available to test. The increase in T_c after additional rounds of processing is consistent with a reduction in film thickness, but the drop in RRR is not expected and may be indicative of film issues introduced by the ashing process.

4 Testing of KIPM detectors at SLAC

Over the last year, we have tested multiple KIPM detectors at SLAC fabricated by the Gowala group at JPL and by myself at Stanford. All devices tested have been based on the 5 GHz KIPM design. A typical cryostat readout setup is shown in figure 2.

The all KIPM detectors tested have been plagued by lower quality factors. Figure 3 shows transmission of a single aluminum KIPM device fabricated by Caltech. Fits to the Lorentzian transmission[4]:

$$t_{21}a(f) = ae^{-2\pi if\tau} \left[1 - \frac{Q_r/Q_c e^{i\phi_0}}{1 + 2iQ(\frac{f-f_r}{f_r})} \right] \quad (1)$$

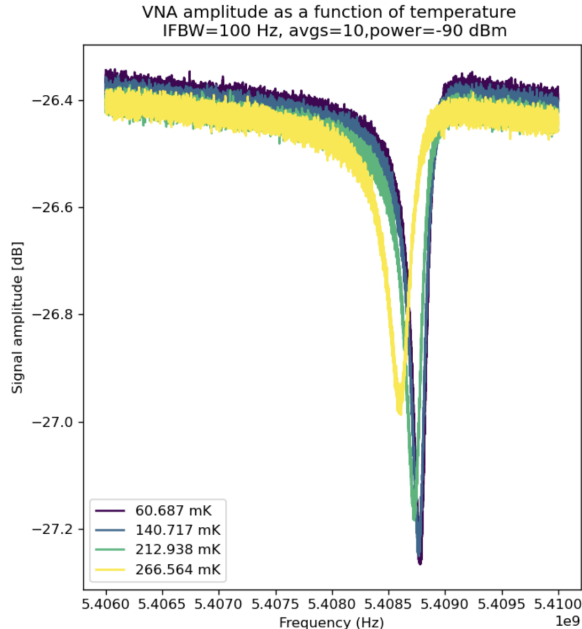


Figure 3: Temperature sweep of the aluminum KIPM detector fabricated at JPL by the Gowala group.

indicates quality factors (Q_r) ranging from 10^3 to 10^4 . This is 10-100x lower than previous, lower frequency KIPM designs fabricated and tested by Caltech and Fermilab [8, 7]

Similarly, an all-aluminum single-kid KIPM detector that was fabricated by myself has a similarly low quality factor of $Q_r = 1700$. With quality factors this low, temperature responses of the KID were likely not achievable at the operating temperature of the dilution refrigerator in which we were operating. In order to characterize the noise performance of these KIPM devices, I am developing a USRP-based readout for low-cost single-resonator testing. This readout system will include a low bandwidth (100 MHz) VNA and two tone IQ streaming using a USRP B205mini-i. In the future, we will use an RFSOC-based readout system under development at SLAC for cosmic microwave background and dark matter detectors.

5 HV-compatible RF housing design

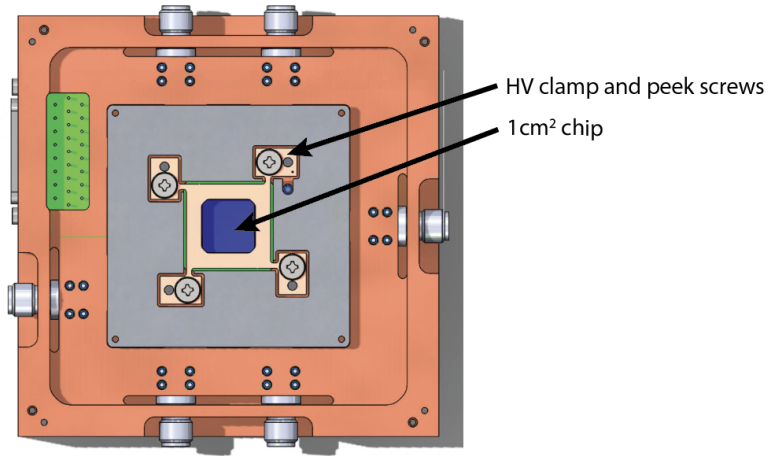
When the fabrication for KIPM detectors and other qubit based phonon sensitive dark matter is at full scale, having a proper RF housing for readout will be imperative. I have spent, in collaboration with Aviv Simchony, a considerable time designing a housing that would fit our specific design requirements. The model is shown in figure 5.

There are many home built and commercial qubit housings used in R&D today, but none have the ability to apply a high voltage (HV) bias to the crystal, while also maintaining minimal contact between the crystal and the housing. This is intended to limit phonon loss from the crystal to the substrate. To accommodate these design requirements, the housing was designed to clamp the chip on the corners using a beryllium coppers spring washers to achieve consistent clamping forces on the chip. The back-plane clamp is designed to hold a high voltage bias, and is electrically insulated using peek screws.

The entire chip and HV clamp is enclosed inside aluminum magnetic shield. Wave guide cutouts are included to complete the co-planar wave-guides on the PCB. The aluminum magnetic shield sits inside a light-tight copper box, that stacks to allow modular assembly and compact installation into a dilution refrigerator. Additionally, the entire housing stack fits within a 5" mu-metal can, to allow for increased magnetic shielding.

The housing includes 6 RF ports, to allow for many configurations of readout and charge bias lines. In addition to the HV bias, there is routing for 22 DC biases to the chip. To accommodate these features, a

(a) Cross sectional view of HV side of qubit housing



(b) Cross sectional view of RF-side of qubit housing

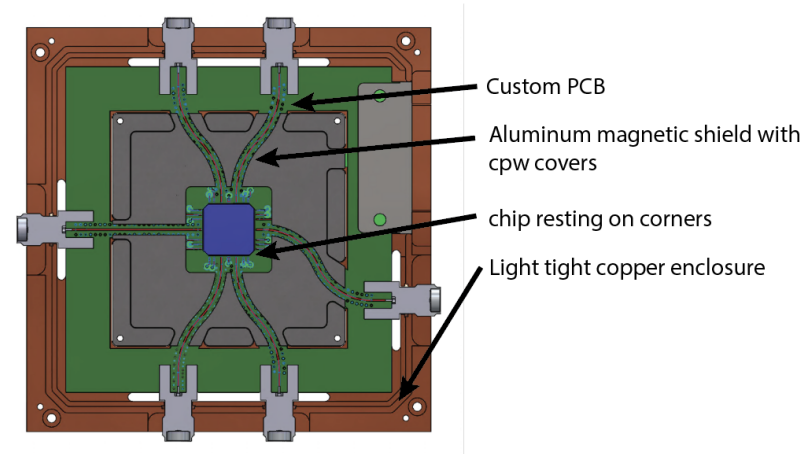


Figure 4: Model of 1cm² RF-HV housing.

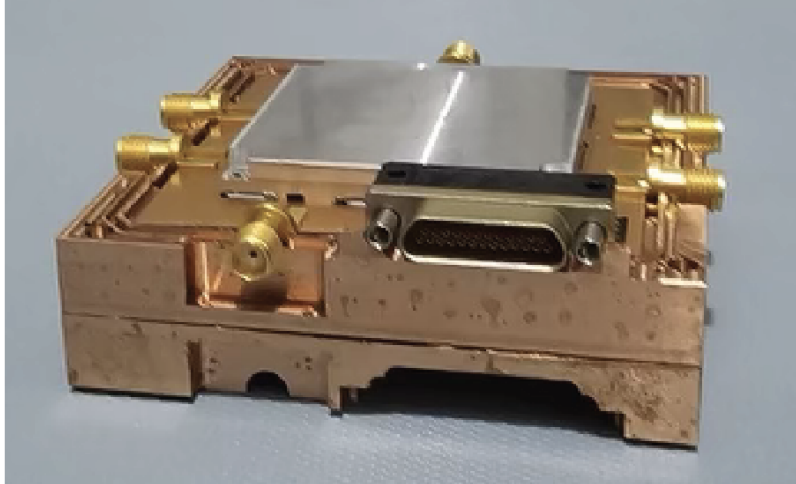


Figure 5: 1cm² RF-HV housing assembled on bench top.

custom 5 layer PCB was designed using Rogers 5870 and FR-4.

The assembled RF-HV housing is seen in figure 5. Testing of the housing using a loop-back chip is imminently planned at SLAC. This will characterize box modes and transmission of all 6 lines. Device testing using KIPM and qubit-based detectors will follow shortly after.

6 Future work and directions

In the near future, I plan on completing the fourth round of fabrication, which will include DC test features to optimize the resonator performance. These features include Van der Pauw probes, 4-wire meanders, and DC inductance structures. Additionally, this round of fabrication includes lower frequency resonator designs which were originally tested by Caltech and shown to have higher Q XXXX. I will also test these resonators using various Aluminum Manganese films. Integration with parametric amplifiers is also underway at SLAC. Future MKIDs will be co-fabricated with transmons in collaboration with Syracuse University to test quasi-particle poisoning.

7 Acknowledgements

I would like to thank Betty Young and Dale Li for their help with process development, and the Irwin group for use of their sputtering system. Additionally, I would like to thank the LINQS group for the use of their e-beam evaporator. The bulk of the fabrication was carried out at the Stanford Nano-fabrication Facility, and I would also like to thank the staff for their valuable help. I would like to thank the SLab group for their testing support and collaboration. Finally, I would like to thank the whole DMQIS group at SLAC for making this work possible.

References

- [1] P. Day et al. “A broadband superconducting detector suitable for use in large arrays”. In: *Nature* 425 (2003), pp. 817–821. DOI: 10.1038/nature02037.
- [2] D. Delicato et al. *Low-energy spectrum of the BULLKID detector array operated on surface*. 2023. arXiv: 2308.14399 [hep-ex].
- [3] Caleb W. Fink et al. *The Superconducting Quasiparticle-Amplifying Transmon: A Qubit-Based Sensor for meV Scale Phonons and Single THz Photons*. 2023. arXiv: 2310.01345 [physics.ins-det].

- [4] Jiansong Gao. “Background Limited Detection and Conformal Mapping”. Dissertation. Pasadena, California: California Institute of Technology, May 2008. DOI: 10.7907/RAT0-VM75. URL: <https://resolver.caltech.edu/CaltechETD:etd-06092008-235549>.
- [5] David Craig Moore. “A Search for Low-Mass Dark Matter with the Cryogenic Dark Matter Search and the Development of Highly Multiplexed Phonon-Mediated Particle Detectors”. Dissertation (Ph.D.) California Institute of Technology, 2012. DOI: 10.7907/X8JD-4R90. URL: <https://resolver.caltech.edu/CaltechTHESIS:05172012-142723949>.
- [6] R. Ren et al. “Design and characterization of a phonon-mediated cryogenic particle detector with an eV-scale threshold and 100 keV-scale dynamic range”. In: *Phys. Rev. D* 104 (3 Aug. 2021), p. 032010. DOI: 10.1103/PhysRevD.104.032010. URL: <https://link.aps.org/doi/10.1103/PhysRevD.104.032010>.
- [7] Dylan J. Temples et al. “Performance of a Kinetic Inductance Phonon-Mediated Detector at the NEXUS Cryogenic Facility”. In: *arXiv preprint* (Feb. 2024). Submitted on 6 Feb 2024. DOI: 10.48550/arXiv.2402.04473. arXiv: 2402.04473 [physics.ins-det]. URL: <https://arxiv.org/abs/2402.04473>.
- [8] Osmond Wen et al. “KID-based phonon-mediated particle detectors”. In: *Proceedings of the LTD20*. Daejeon, Korea, July 2023.
- [9] Jonas Zmuidzinas. “Superconducting Microresonators: Physics and Applications”. In: *Annual Review of Condensed Matter Physics* 3.1 (2012), pp. 169–214. DOI: 10.1146/annurev-conmatphys-020911-125022. eprint: <https://doi.org/10.1146/annurev-conmatphys-020911-125022>. URL: <https://doi.org/10.1146/annurev-conmatphys-020911-125022>.